

UC Irvine

UC Irvine Previously Published Works

Title

Location change method for imaging chemical reactivity and catalysis with single-molecule and -particle fluorescence microscopy

Permalink

<https://escholarship.org/uc/item/1tj4z7rq>

Journal

Physical Chemistry Chemical Physics, 16(31)

ISSN

0956-5000

Author

Blum, SA

Publication Date

2014-08-21

DOI

10.1039/c4cp00353e

Copyright Information

This work is made available under the terms of a Creative Commons Attribution License, available at <https://creativecommons.org/licenses/by/4.0/>

Peer reviewed

Location change method for imaging chemical reactivity and catalysis with single-molecule and -particle fluorescence microscopy

Cite this: *Phys. Chem. Chem. Phys.*, 2014, 16, 16333

S. A. Blum

In the last eight years, it has become possible to image chemical reactivity at the single-molecule and -particle level with fluorescence microscopy. This Perspective describes one of the imaging techniques that enabled this state-of-the-art application: imaging by the location change of molecules and particles. In this method, the microscope and experiment are configured to produce a signal when an individual molecule or particle changes location or changes mobility concurrently with a chemical change. This imaging technique has enabled observation of single chemical reactions and unraveled mechanisms of complex chemical and physical processes in transition metal and polymerization systems. This Perspective has three major goals: (1) to unify studies of different chemical processes or of different chemical questions, which, in spite of these differences, employ a similar microscopy detection method, (2) to explain the technique to nonexperts and those who might be interested in joining this nascent field, and (3) to highlight unique information available through this cross-disciplinary technique and the value this information has for chemical reaction development generally and catalysis specifically. To this end, application of the location change method to the investigation of polymerization reactions with radical initiators and separately with metal catalysts, and to ligand exchange reactions at platinum complexes are described.

Received 23rd January 2014,
Accepted 25th March 2014

DOI: 10.1039/c4cp00353e

www.rsc.org/pccp

Introduction

Of critical importance for understanding chemical processes are in operando analytical techniques that operate under conditions similar to those for synthetic chemistry: condensed phase, ambient or selectable temperatures, and “dirtiness” inherent to everyday chemistry (*e.g.*, rough surfaces, standard levels of impurities, heterogeneous reactivity distributions).^{1–4} As in operando detection with fluorescence microscopy reaches the ultimate sensitivity limit of individual molecules and particles—and now of individual chemical reactions—an increasing number of chemists are designing experiments to garner unique insights into catalysis and stoichiometric reactivity *via* this technique. Identification of the active phase of the catalyst in ruthenium-catalyzed polymerization,⁵ mechanisms responsible for polymer morphology,⁶ local environments in radical polymerization,^{7,8} crystal face selectivity in surface hydrolysis of esters,⁹ mechanistic steps in epoxidation of olefins,^{10,11} heterogeneous reactivity of gold nanocatalysts,^{12–16} protonation of amines,¹⁷ surface spatial distribution with kinetics of ligand exchange reactions at platinum,^{18–22} and ordering within nanomaterials²³ have provided the first applications in purely chemical systems unrelated to biology.²⁴

In order to image a chemical process, however, this chemical process needs to result in a change in fluorescent output that is detectable. This is an area where chemists recently have made fundamental enabling advances.⁴ In the past eight years, two methods have been designed to detect a fluorescence change upon chemical reactivity: a color change method and a location change method.⁴ This Perspective focuses on explaining one of these, the location change method.

This description targets nonexperts across multiple traditionally separate scientific disciplines, including synthetic chemists, biophysicists, and physical chemists. A goal of this Perspective is to enable scientists from areas that do not traditionally use imaging techniques to understand—and perhaps even adopt—this method with its unique insights into chemical reactivity.

To achieve this goal, the setup of the microscope and example chemical systems are described. Five examples of information about chemical processes that would not be obtainable by traditional ensemble techniques but were obtained through the location change single-molecule and -particle imaging method are described. This Perspective aims to be authoritative, with all needed information for casual readers to understand the method provided in one article, and balanced, by describing context where this method fits with other methods of single-molecule and -particle fluorescence imaging of chemical processes.

Chemistry Department, University of California, 1102 Natural Sciences 2, Irvine, CA 92697-2025, USA. E-mail: blums@uci.edu

Microscope setup: TIRF and wide-field epifluorescence

A. Basic microscope setup and definition of terms

Like other types of fluorescence imaging, single-molecule and -particle fluorescence microscopy requires an excitation source. The high intensity of light from (and thus high fluorescence signal from) a laser makes it the excitation source of choice to this high-sensitivity technique. Two options for the direction in which the laser beam is pointed provide two configurations: wide-field epifluorescence and total internal reflectance fluorescence (TIRF).²⁵ Both configurations are well established for imaging in biophysical systems,²⁶ but have only recently seen application to chemical systems outside of biology. Both configurations have been employed for location change imaging in chemistry. The primary difference between these two configurations is the depth above the glass coverslip that is excited. Each configuration therefore accesses somewhat different information about the chemical sample, as will now be described.

Wide-field epifluorescence configuration. In this configuration, the laser points straight up into the reaction chamber (Fig. 1a). The outcome of this laser position is that the entire column of solution directly above the laser is illuminated. Thus, fluorescent molecules and particles present in this column are excited and fluoresce. Fluorescent molecules or particles that are freely diffusing, however, are moving significantly faster than the data collection and therefore are imaged as only a background hazy glow. Molecules or particles that are experiencing sufficiently slow diffusions are imaged as distinct single species. Chemical reactions that increase the size of the molecules and particles (e.g., polymerization) produce larger products that diffuse more slowly than starting materials.

TIRF (total internal reflection fluorescence) configuration. In this configuration, the laser points at an angle to the reaction chamber (Fig. 1b). At this angle, the glass coverslip bottom of the reaction chamber acts similar to a fiber optic cable in that laser light remains contained inside the glass coverslip and does not escape. The outcome of this laser position is that the solution above the laser is not illuminated. Fluorescent molecules and particles that are very close to the glass, however, are excited through a tunnelling process classically known as the evanescent wave.²⁵ The probability of this tunnelling and excitation decays exponentially. Therefore a practical limit for excitation and imaging is about 50–200 nm beyond the surface of the glass, depending on the brightness of the object.²⁵

Because only fluorophores near the glass coverslip are close enough to be excited, there is only a small depth of the background solution being excited. This location selective excitation makes TIRF particularly suited to high signal-to-background imaging of single molecules or particles attached to the glass coverslip.

In the TIRF configuration, akin to the wide-field epifluorescence configuration, imaging relies on a product that has changed location and is differently mobile when compared to the starting material. In theory, this difference in mobility could be either a freely diffusing starting material and an anchored-to-glass product

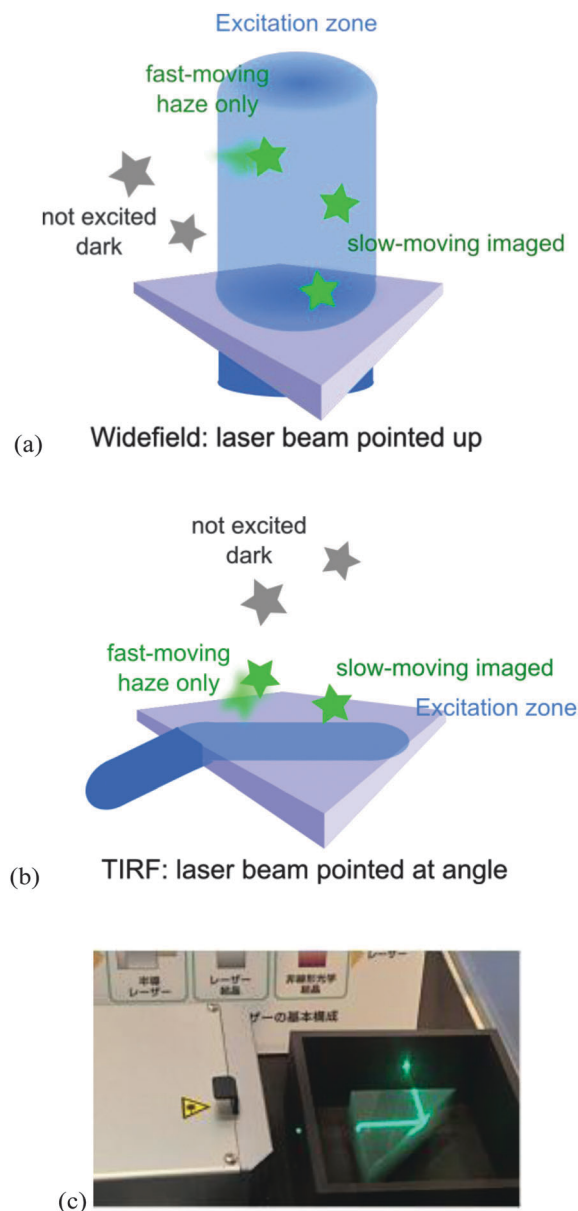


Fig. 1 (a) Schematic of wide-field epifluorescence imaging. Laser beam (blue) is pointed up into sample and excites molecules at an above the glass coverslip (grey) causing them to fluoresce (green); molecules that are diffusing quickly are excited but are not resolved and appear as a background haze. (b) Schematic of TIRF imaging. Laser beam (blue) enters glass coverslip (grey) at an angle that produces total internal reflection. Molecules that are less than ~ 200 nm above the surface are excited causing them to fluoresce (green). Similar to wide-field epifluorescence, in TIRF molecules that are diffusing quickly are excited but are not resolved and appear as a background haze. (c) An example of total internal reflection (TIR) with a prism and a green laser beam, from a science exhibit for general audiences at RIKEN in Tokyo, Japan.

or *vice versa* with an anchored-to-glass starting material and freely diffusing product; in practice, however, only the former option has been employed to date in published studies. There are challenges with both approaches: with a freely diffusing starting material approach, care must be taken to assign location changes to chemical processes rather than nonspecific

attractive interactions like physisorption. With a freely diffusing product approach, care must be taken to assign this disappearance with chemical change rather than other processes such as quenching or photobleaching that would also cause disappearance of the signal from the originally tethered molecule. Physical or chemical attachment of only the product and not the starting material to the glass^{5,6,18–21} or changes in local viscosity within a reaction medium⁷ have been employed to achieve this difference in diffusion rate.

B. Comparison of concepts: location change imaging and color change imaging methods

Location change imaging employs the change in location or change in the movement ability of the molecule or particle as a tool to image a chemical process. The location change method differs from the color change method in that the chemical structure of the fluorophore itself remains unchanged. Thus, the fluorophore has similar photophysical properties before and after the chemical reaction; only its location has changed. In this way, the fluorophore is a spectator in the chemical process rather than a participant. In contrast, the color change methods so far reported involve a chemical change to the backbone of the fluorophore that creates a different photophysical properties resulting in a color change or a quantum yield change from low (zero to no color) to high (color) before and after the chemical reaction.

C. Time resolution

In published examples of imaging chemical processes at the single-molecule and -particle level, the time resolution is limited by camera technology. The time resolution in this context is reflected in the exposure time per frame, which at the practical limit is the amount of time that it takes the camera to gather enough photons from a single molecule or particle to accurately image that signal over equipment noise and over the fluorescent background of the sample. Published examples of location change imaging have reported time resolutions between 300 ms to 38 ms (*i.e.*, 300–38 ms per frame of a timelapse movie of a chemical process).^{7,18}

The current technology-limited time resolution differs from the ultimate theoretical time resolution limit in nature, which is the fluorescence lifetime of a single fluorophore (*i.e.*, the time for one fluorophore to emit). The fluorescence lifetime for typical small organic molecules is on the order of nanoseconds. Therefore, there is reason to anticipate that time resolution in single-molecule and -particle fluorescence microscopy will continue to increase as technology improves.

Examples of chemical information available through the location change method that is not available through traditional ensemble measurements

Single-molecule and -particle microscopy techniques provide complementary information to that from ensemble measurements. The main differences are that single-molecule and -particle microscopy

techniques can monitor how the same individual molecule or particle behaves with time, and determine the location of molecules and particles relative to each other or to other objects. Thus, these techniques do not lose information due to the ensemble averaging inherent to traditional techniques like NMR, IR, or UV-vis spectroscopy. These traditional techniques, in contrast, measure the average properties of micro-moles of molecules.

Acquired *via* location change fluorescence microscopy methods, this unique information has been used to reveal mechanistic information about radical and transition-metal catalyzed polymerization and surface special distributions metal ligand exchange. In each case, the information revealed would not have been available through a traditional ensemble technique. Five illustrative examples of data and understanding of chemical systems generated by location change imaging now will be described in sections A–E, below.

A. Mechanistic origin of polymer morphology

Global interest in catalysis. Polymers are workhorse materials. The macroscopic properties of a polymer, *e.g.*, its flexibility, melting point, chemical degradation, and optical characteristics, are determined partially by the microscopic arrangements of individual polymer strands. Multiple physical and chemical processes over the course of the reaction often determine this polymer morphology. Identification of the steps involved in these processes, their relative rates, and the mechanisms through which they dictate polymer morphology are therefore central for creating polymerization catalysts that produce materials of desired properties.

This study. Established a single-particle and -molecule fluorescence imaging technique to address these questions. This imaging revealed a precipitation polymerization process, the relative rates of certain chemical and physical steps, and an aggregation mechanism responsible for “dumbbell” polymer morphology in the polymerization of dicyclopentadiene catalysed by a ruthenium carbene complex, Grubbs 2nd generation catalyst.^{5,6} This information was obtained because of the ability of the technique to probe individual polymer particles.

The imaging concept harnessed a location change that resulted in the difference in diffusion rates between the starting monomer dicyclopentadiene (**1**) and starting small-molecule fluorescent probe (**2**) (both small and therefore fast) and the precipitated product probe-tagged polymer (large and precipitated onto glass coverslip and therefore slow or stationary) (Fig. 2; top equation with green only). Data was obtained under both wide-field epifluorescence fluorescence and TIRF configurations.

At the initiation of the reaction, monomer **1** and the green boron dipyrromethene (BODIPY) probe **2** are in solution above the glass surface and rapidly diffusing, therefore they are not resolved as individual molecules (*vide infra*). Catalyst **4** is in solution but not tagged with a fluorophore, and therefore is not observed by this technique. During progression of the reaction, aggregates of polydicyclopentadiene reach the size for insolubility in the medium and precipitate onto the glass as larger particles (<500 nm to 5 μm) which are then observed.

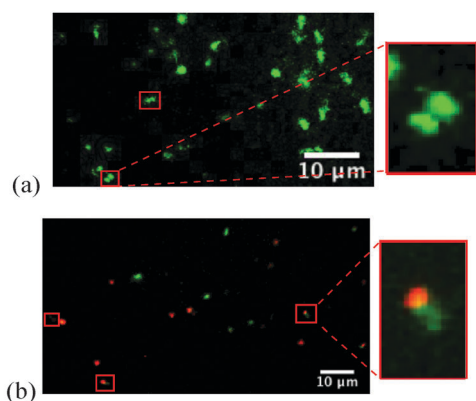
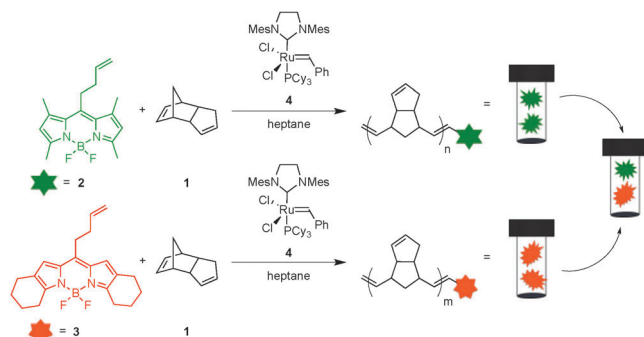


Fig. 2 Experiment schematic. In operando microscopy imaging of phase separation in DCPD polymerization. Reproduced from ref. 2. (a) Fluorescence microscopy image of DCPD polymerization at $t = 187$ s showing dumbbell morphology of polymer particles (examples in red boxes). (b) Mixing experiment of DCPD polymerization using both fluorophores **2** and **3** revealed that aggregation of two preformed polymer particles is responsible for the dumbbell formation.

By this technique, it was identified for the first time that these precipitated polymers have two-lobe shapes, akin to colloquial “dumbbells” (Fig. 2a). A two-color mixing experiment revealed the mechanistic origin of this morphology: the two lobes of the dumbbell form independently and then aggregate together. In the two-color experiment, polymerization was initiated in two separate vials simultaneously: one vial with green BODIPY **2** and a separate vial with orange BODIPY **3**. After 2 minutes, these solutions were mixed together in one microscope reaction chamber (Fig. 2, reactions depicted as green and orange equations initiated separately and then mixed).

Images of the subsequent precipitation of polydicyclopentadiene in the microscope reaction chamber are shown in Fig. 2b. The presence of lobes of green attached to lobes of orange demonstrated that aggregation is responsible for generating the morphology, because independently formed green and orange lobes, originally formed in separate vials, associated together after mixing.

B. Timestamp or “pulse/chase” experiments: at what time in the reaction was a specific polymer synthesized?

Global interest in catalysis. Efficient catalysts exhibit high selectivity for the desired product. The structure of the catalyst

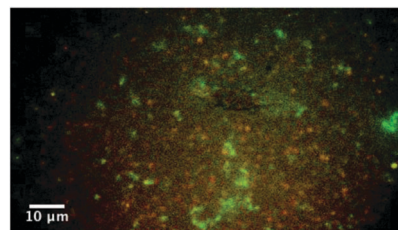


Fig. 3 Timestamp or “pulse-chase” experiment with green and orange fluorescent polymers in same sample. Color of polymer particle indicates time of chemical synthesis, with green polymers synthesized at earlier reaction stages (<2.4 min) and orange polymers synthesized at later reaction stages (>2.4 min). Reproduced from ref. 2.

can change over the course of the reaction—sometimes to degrade, sometimes to reveal a more selective catalyst after an induction period. The ability to determine the time at which an individual product molecule of particular selectivity formed would allow more accurate modelling of the structure of the catalyst at that time.

This study. Single-particle fluorescence microscopic imaging permitted the identification of the time of formation of individual particles of polymer in this proof-of-concept study. These polymer particles were formed during the course of the ruthenium-catalyzed polymerization reaction described in Fig. 3.

Specifically, a timestamp or “pulse/chase” experiment swapped the solution of green BODIPY probe for a solution of orange BODIPY probe after 2.4 minutes of reaction. Otherwise identical polymers then could be identified by color as has having formed early in the reaction (green) or later in the reaction (orange) regardless of when the polymer precipitated (Fig. 3). In this way, the ability to determine the timing of the chemical reaction that resulted in polymerization of an individual polymer molecule was decoupled from the timing of the observed physical precipitation process.

C. Detection of local environment heterogeneities on molecular level during radical polymerization

Global interest in catalysis. Synthesis of polymers with specific bulk properties is an international industry. The bulk properties of the synthesized polymer are influenced by microscopic heterogeneities, yet most common analytical techniques for interrogating polymer properties miss these local heterogeneities because they instead provide information on the average properties of the bulk material. The ability to detect and measure these local heterogeneities, and subsequently to determine the influence of reaction conditions on the microscopic structure of the polymer, therefore provide unique opportunities for reaction optimization.

This study. During the course of a bulk radical polymerization reaction of styrene, the degree of crosslinked polystyrene was monitored by single-molecule fluorescence microscopy to reveal local differences.⁷ Fluorescent perylenediimide probe molecules (**5**), initially freely diffusing, became physically trapped by the growing polymer over the course of the experiment.

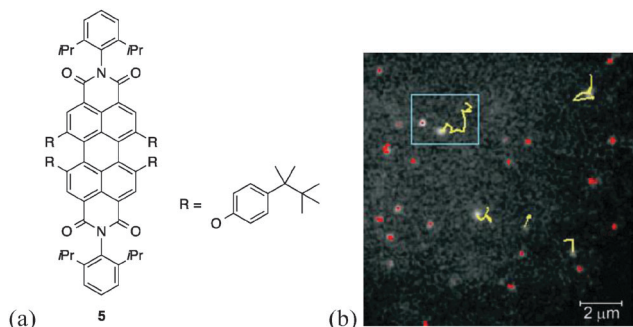


Fig. 4 (a) Probe molecule **5**, which becomes physically entrapped in crosslinked polystyrene as polymerization proceeds. (b) Diffusion of about 25 probe molecules represented by color in this $\sim 10 \mu\text{m} \times 10 \mu\text{m}$ wide-field epifluorescence image: immobile probes shown in red; slowly diffusing probes shown in yellow with superimposed paths; and fast diffusing probes appear as a grey background haze. Reproduced from ref. 3.

Therefore, the mobility of the probe molecules decreased with the degree of polymerization. The mobility of an individual probe molecule informed on the degree of polymerization in its local environment. Data reproduced in Fig. 4 was obtained under the wide-field epifluorescence configuration.

The mobility of individual probe molecules was quantified as their diffusion rate. Fig. 4b shows example path lengths of slowly diffusing probe molecules in yellow. These probes indicate moderate degrees of local polymerization. Probe molecules that were effectively stationary during the experiment, indicating high levels of local polymerization, are shown in red. Differences in diffusion rates expose the differences in the degree of polymer network at that location at a given point in time during the polymerization reaction. In contrast, detection of this heterogeneity would be obscured by the average diffusion measurements available from traditional ensemble viscosity measurements using the Stokes–Einstein relation.

D. Determining the phase of the active ruthenium polymerization catalyst: homogeneous, heterogeneous, or both?

Global interest in catalysis. Improvement of catalytic reactions relies on accurate knowledge of the structure of the active catalyst. This structure is employed to model catalyst–substrate interactions which then are applied to modify the structure of the catalyst to optimize the efficiency of the reaction. This efficient path to optimization critically depends on the initial correct determination of the active catalyst—a long standing challenge in chemistry.

This study. Determined that the active catalyst in a widely used polymerization system is exclusively homogeneous through fluorescence microscopy imaging; as the first such application, it demonstrated a new analytical tool for chemists to address this long-standing challenge of catalyst identification. Specifically, the location change microscopy method was employed to image the location of nascent polymers relative to a solid surface of a crystal of ruthenium metathesis catalyst at early reaction stages.⁵ In this way, the early stage polymers could

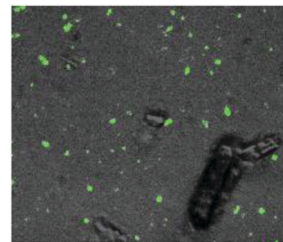


Fig. 5 The location of newly formed polymers (green) indicates that they are not colocalized with the surface of a crystal of Grubbs II ruthenium catalyst (black). Instead, they are distributed on the glass coverslip surface. This spatial distribution demonstrates that these polymers formed *via* homogenous catalysis in solution, rather than heterogeneous catalysis at the solution/crystal surface interface. Reproduced from ref. 1.

be probed for their location: on the crystals (growing from them, heterogeneous catalysis) or in solution (homogenous catalysis). For these studies, a similar set of probe molecules and reaction conditions was employed as in Fig. 2 (*vide infra*). In this set of experiments the location of individual crystalline particles of solid **4** were observed by ambient-light imaging, and compared with the location of the polymers at early reaction stages.

Specifically, BODIPY fluorophore probe **2** was added to a polymerization reaction of dicyclopentadiene **1** *via* Grubbs II catalyst **4**. The probe molecule contained a tethered olefin, which became incorporated into the growing polymer chain as depicted previously in Fig. 2. This incorporation permitted imaging of the polymer when the polymers reached a size for slower diffusion or became stationary by virtue of attachment to the crystal or glass surfaces.

The spatially resolved location data available through this technique showed that these early stage polymers did not form on the surface of the crystals, but rather in solution above the microscope glass coverslip. These polymers then precipitated onto the surface of the glass and became stationary, where they were observed. Fig. 5 shows a $52 \times 52 \mu\text{m}^2$ frame from the reaction movie; green spots are individual particles of polydicyclopentadiene at early reaction stages. As can be seen in Fig. 5, these particles are not associated with—and thus not growing from—the surface of the crystal of ruthenium catalyst. Thus, data available through this technique demonstrates that the polydicyclopentadiene is formed by homogenous solution-phase catalysis only; no evidence for heterogeneous catalysis at the crystal surface/solution interface was observed in this system.

E. Superlocalization, subensemble kinetics, and surface spatial distribution of platinum-sulfur ligand exchange reactions

Global interest in catalysis. As reactions progress on a surface, the chemical environment of that surface changes. This change raises the possibility that catalytic surfaces may become more or less active over the course of their employment. Information on the molecular basis for reactivity changes is therefore critical for the optimization of catalytic surfaces.

This study. The ability to localize individual chemical reactions on a functionalized surface permitted the probing of whether or

not ligand exchange reactions at individual platinum centers were correlated, *i.e.*, whether or not the chemical reaction of one platinum complex influenced the location of a future chemical reaction.^{18–21} This molecular interaction could provide a basis for changes in surface reactivity over time. The surface in this study was modified silica, a common support for industrial catalysts. The ligand-exchange reactions were found to be uncorrelated on the examined length scales, *i.e.*, the chemical reaction of one platinum complex did not influence the location of a future ligand exchange reaction. This information would not be available through ensemble analytical techniques.

Specifically, the ability to localize, or determine the *x,y* (and sometimes *z*) location of, single molecules is no longer diffraction limited. Localization to distances smaller than the diffraction limit of light, or superlocalization, has become possible and now, arguably, routine^{27,28} due excellent contributions from the biophysical community.^{29,30} Superlocalization fundamentals and applications to biology have been extensively reviewed elsewhere.^{27,28} This section therefore provides a targeted example of its application to location change monitoring of chemical reactions rather than an in-depth review.

Superlocalization was applied to determine the *x,y* position of several hundred platinum complexes that were products of ligand exchange reactions after in operando imaging of the individual events (Fig. 6).¹⁹ Specifically, platinum–water complex **6**, labelled with a green BODIPY probe, freely diffused in a water–acetone solution prior to a ligand exchange reaction.^{18–20} A chemical exchange of the water ligand for a surface-bound thiourea ligand, however, resulted in a location change of the platinum complex through immobilization of the platinum centre to the glass as surface-bound complex **7**, thus changing the location of its tethered BODIPY probe as well.

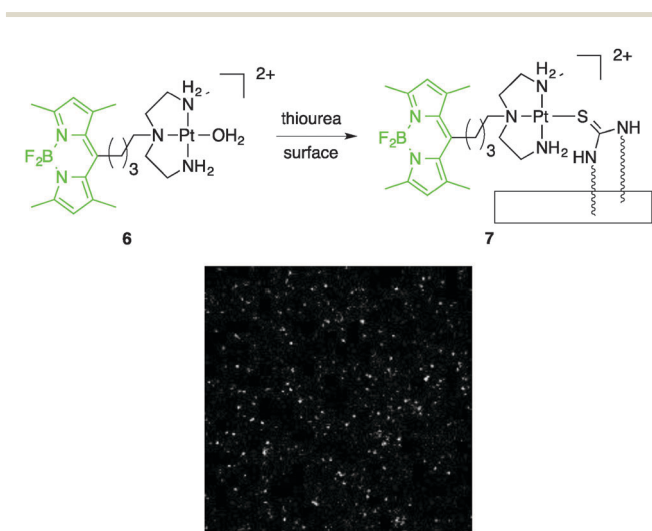


Fig. 6 Top: ligand exchange chemical reaction equation. Bottom: TIRF image of a $52 \times 52 \mu\text{m}^2$ region of the thiourea-functionalized glass surface. Single platinum complexes (**7**) that are the products of individual ligand exchange reactions appear as white spots. The surface location of one reaction could be localized with positional accuracy of up to ± 11 nm. Reproduced from ref. 14.

The accuracy of superlocalization measurements depends on the brightness of the signal over background, and the brightest signals produce the most accurate location data. The location of an individual ligand exchange chemical reaction could be determined with a positional accuracy of up to ± 11 nm. This data therefore provided information about the spatial distribution of ligand exchange reactions on the chemically modified glass surface with subdiffraction accuracy. This data also enabled acquisition of subensemble kinetics of small numbers of ligand exchange reactions on specific surface regions, data that showed that different regions of the surface displayed different subensemble kinetics.²⁰ As part of this study, a process to increase accuracy of single-molecule kinetics measurements was also developed, which accounts for some of the molecules to be in temporary dark (nonfluorescent) states from surface quenching and long-lived triplet states. Because superlocalization and superresolution techniques continue to increase in positional accuracy, it will be possible to probe this question at shorter and shorter distances in the future—perhaps reaching the ultimate accuracy of the dimensions of one molecule or even a part of one molecule.

Conclusions

The past eight years have seen the initiation of studying chemical systems outside of biophysics by single-molecule and -particle fluorescence microscopy. Two general methods have emerged to generate a fluorescent signal that indicates a chemical process: location change imaging and color change imaging. This Perspective explains the location change imaging method and describes some of the exciting insights into chemical reactivity provided through its application. It is an ultimate example of a cross-disciplinary field, bringing together techniques, equipment, and expertise from biophysics, physical, organic, inorganic, and mechanistic chemistry, materials engineering, and catalysis. The future is bright for this and other single-molecule and -particle fluorescence microscopy methods to unravel complex chemical processes.

Acknowledgements

SAB thanks the U.S. Department of Energy, Office of Basic Energy Sciences for funding (DE-FG02-08ER15994).

Notes and references

- 1 R. H. Crabtree, *Chem. Rev.*, 2012, **112**, 1536–1554.
- 2 I. L. C. Buurmans and B. M. Weckhuysen, *Nat. Chem.*, 2012, **4**, 873–886.
- 3 I. L. C. Buurmans, J. Ruiz-Martinez, W. V. Knowles, D. v. d. Beek, A. A. Bergwerff, E. T. C. Vogt and B. M. Weckhuysen, *Nat. Chem.*, 2011, **3**, 862–867.
- 4 T. Cordes and S. A. Blum, *Nat. Chem.*, 2013, **5**, 993–999.
- 5 N. M. Esfandiari and S. A. Blum, *J. Am. Chem. Soc.*, 2011, **133**, 18145–18147.

- 6 E. M. Hensle and S. A. Blum, *J. Am. Chem. Soc.*, 2013, **135**, 12324–12328.
- 7 D. Woll, H. Uji-i, T. Schnitzler, J. Hotta, P. Dedecker, A. Herrmann, F. C. De Schryver, K. Müllen and J. Hofkens, *Angew. Chem., Int. Ed.*, 2008, **47**, 783–787.
- 8 D. Woll, E. Braeken, A. Deres, F. De Schryver, H. Uji-i and J. Hofkens, *Chem. Soc. Rev.*, 2009, **2**, 313–328.
- 9 M. B. J. Roefsaers, B. F. Sels, H. Uji-i, F. C. De Schryver, P. A. Jacobs, D. E. De Vos and J. Hofkens, *Nature*, 2006, **439**, 572–575.
- 10 M. B. J. Roefsaers, G. De Cremer, J. Libeert, R. Ameloot, P. Dedecker, A.-J. Bons, M. Bückins, J. A. Martens, B. F. Sels, D. E. De Vos and J. Hofkens, *Angew. Chem., Int. Ed.*, 2009, **48**, 9285–9289.
- 11 A. Rybina, C. Lang, M. Wirtz, K. Grussmayer, A. Kurz, F. Maier, A. Schmitt, O. Trapp, G. Jung and D.-P. Hertzen, *Angew. Chem., Int. Ed.*, 2013, **52**, 6322–6325.
- 12 W. Xu, J. S. Kong and P. Chen, *Phys. Chem. Chem. Phys.*, 2009, **11**, 2767–2778.
- 13 X. Zhou, W. Xu, G. Liu, D. Panda and P. Chen, *J. Am. Chem. Soc.*, 2010, **132**, 138–146.
- 14 K. S. Han, G. Liu, X. Zhou, R. E. Medina and P. Chen, *Nano Lett.*, 2012, **12**, 1253–1259.
- 15 N. M. Andoy, X. Zhou, E. Choudhary, H. Shen, G. Liu and P. Chen, *J. Am. Chem. Soc.*, 2013, **135**, 1845–1852.
- 16 P. Chen, X. Zhou, H. Shen, N. M. Andoy, E. Choudhary, K. S. Han, G. Liu and W. Meng, *Chem. Soc. Rev.*, 2010, **39**, 4560–4570.
- 17 R. Ameloot, M. B. J. Roefsaers, M. Baruah, G. De Cremer, B. Sels, D. De Vos and J. Hofkens, *Photochem. Photobiol. Sci.*, 2009, **8**, 453–456.
- 18 N. M. Esfandiari, Y. Wang, J. Y. Bass, T. P. Cornell, D. A. L. Otte, M. H. Cheng, J. C. Hemminger, T. M. Mcintire, V. A. Mandelshtam and S. A. Blum, *J. Am. Chem. Soc.*, 2010, **132**, 15167–15169.
- 19 N. M. Esfandiari, Y. Wang, T. M. McIntire and S. A. Blum, *Organometallics*, 2011, **30**, 2901–2907.
- 20 N. M. Esfandiari, Y. Wang, J. Y. Bass and S. A. Blum, *Inorg. Chem.*, 2011, **50**, 9201–9203.
- 21 S. M. Canham, J. Y. Bass, O. Navarro, S.-G. Lim, N. Das and S. A. Blum, *Organometallics*, 2008, **27**, 2172–2175.
- 22 S.-G. Lim and S. A. Blum, *Organometallics*, 2009, **28**, 4643.
- 23 B. Scheinhardt, J. Trzaskowski, M. C. Baier, B. Stempfle, A. Oppermann, D. Wöll and S. Mecking, *Macromolecules*, 2013, **46**, 7902–7910.
- 24 Some chemical reactions have been studied in biomolecular/biophysical systems, like individual DNA copper binding events and single ATP turnover leading to enzymatic motion, for examples see: (a) A. Sprodefeld, A. Kiel, D.-P. Hertzen and R. Kramer, *Z. Anorg. Allg. Chem.*, 2013, **639**, 1636–1639; (b) A. Yildiz, M. Tomishige, R. D. Vale and P. R. Selvin, *Science*, 2004, **303**, 676–678.
- 25 D. Axelrod, *Methods Enzymol.*, 2003, **361**, 1–133.
- 26 A. Yildiz, M. Tomishige, R. D. Vale and P. R. Selvin, *Science*, 2004, **303**, 676–678.
- 27 M. Sauer, *J. Cell Sci.*, 2013, **126**, 3505–3513.
- 28 L. Schermelleh, R. Heintzmann and H. Leonhardt, *J. Cell Biol.*, 2010, 165–175.
- 29 For a representative example, see: E. Betzig, G. H. Patterson, R. Sougrat, O. W. Lindwasser, S. Olenych, J. S. Bonifacino, M. W. Davison, J. Lippincott-Schwartz and H. B. Hess, *Science*, 2006, **313**, 1642–1645.
- 30 For a representative example, see: S. Berning, K. I. Willig, H. Steffens, P. Dibaj and S. W. Hell, *Science*, 2012, **335**, 551.